Smart Antennas for Combined DOA and Joint Channel Estimation in Time-Slotted CDMA Mobile Radio Systems with Joint Detection

Josef Johannes Blanz, Apostolos Papathanassiou, Martin Haardt, *Senior Member, IEEE*, Ignasi Furió, *Senior Member, IEEE*, and Paul Walter Baier, *Fellow, IEEE*

***Abstract*—In cellular mobile radio systems, the directional inhomogeneity of the mobile radio channel can be exploited by smart antennas to increase the spectral efficiency. In this paper, a novel smart antenna concept applying receiver antenna diversity at the uplink receiver is investigated for a time-slotted code-division multiple-access (CDMA) mobile radio air interface termed time-division CDMA (TD-CDMA), which has been selected by the European Telecommunications Standards Institute (ETSI) in January 1998 to form part of the Universal Mobile Telecommunications System (UMTS) air interface standard. First, a combined direction-of-arrival (DOA) and joint channel estimation scheme is presented, which is based on DOA estimation using the Unitary ESPRIT algorithm and maximum likelihood estimation of the channel impulse responses associated with the estimated DOA's, which can also be used as an input for advanced mobile positioning schemes in UMTS. The performance of the combined DOA and joint channel estimation is compared with the conventional channel estimation through simulations in rural and urban propagation environments. Moreover, a novel joint data detection scheme is considered, which explicitly takes into account the signal DOA's and the associated channel impulse responses. The link level performance of a TD-CDMA mobile radio system using these novel schemes is evaluated by Monte Carlo simulations of data transmission, and average bit error rates (BER's) are determined for rural and urban propagation environments. The simulation results indicate that, depending on the propagation environment, the exploitation of the knowledge of the directional inhomogeneity of the mobile radio channel can lead to considerable system performance enhancements.**

***Index Terms*—Channel estimation, direction-of-arrival estimation, Monte Carlo simulations, smart antennas, time-slotted CDMA.**

I. Introduction

AT PRESENT, smart antenna concepts applicable at the base stations (BS's) of cellular mobile radio systems are the subject of worldwide research activities [1]–[5]. Taking advantage of the directional inhomogeneity of the mobile radio channel [2], [5], the application of smart antennas is expected to allow an increase of the admissible number of users and a decrease of both the cluster order and the transmission powers. Smart antennas consist of an antenna array and means for processing the output signals of the array elements. Among various smart antenna concepts, receiver antenna diversity techniques are especially attractive because only the signal processing at the receiver has to be adapted, whereas the transmission scheme can remain unchanged [3], [6]. In this paper, a smart antenna concept based on a combined direction-of-arrival (DOA) and joint channel estimation scheme is investigated for a time-slotted code-division multiple-access (CDMA) mobile radio system applying joint data detection at the uplink receiver [7], [8]. It is noted that a similar technique for jointly estimating the DOA's and path delays for single-user time-division multiple-access (TDMA) is proposed in [9]–[11]. In the present work, it is assumed that the channel impulse response associated with a certain DOA can have a large delay spread. In order to estimate these channels, the channel impulse responses for the links between the transmitters and each of the array elements are estimated in a first step, as it is done in [6]. In a second step, DOA's of waves carrying signals transmitted by the users assigned to the considered BS are estimated based on said channel impulse response estimates. The information about the DOA's of the impinging wavefronts can be exploited in order to estimate the channels associated with the different DOA's. Thus, this novel approach provides an enhanced channel estimation, which improves the channel impulse response estimates determined in the first step. In this way, the directional inhomogeneity of the mobile radio channel is exploited, since the actual channel impulse responses are estimated and not the links between every user and each array element, as it is done in [6]. Furthermore, a novel joint data detection scheme will be presented, which is based on the above-mentioned improved channel impulse response estimates and their corresponding DOA's. This technique can be considered as an extension of the zero forcing block linear equalizer (ZF-BLE) [6], [8].

The considered time-slotted CDMA mobile radio air interface—selected by the European Telecommunications Standards Institute (ETSI) to form part of the Universal Mobile Telecommunications System (UMTS) air interface standard—is termed time division CDMA (TD-CDMA) and is based on an F/TDMA scheme which is extended by a supplementary CDMA component [8], [13]. In the same frequency band and time slot, K

Manuscript received July 1, 1997; revised February 5, 1999. This work was supported by a research grant under the *Schwerpunktprogramm Mobilkommunikation* by the German Research Society (DFG) and by the Supercomputer Staff at the Regionales Hochschulrechenzentrum Kaiserslautern (RHRK), Germany.

J. J. Blanz is with Qualcomm, Inc., Boulder, CO 80301 USA.

A. Papathanassiou, I. Furió, and P. W. Baier are with the Research Group for RF Communications, University of Kaiserslautern, D-67653 Kaiserslautern, Germany (e-mail: papa@rhrk.uni-kl.de).

M. Haardt is with SIEMENS AG, OEN MN P 36, D-81359 Munich, Germany.

Publisher Item Identifier S 0018-9545(00)02578-0.

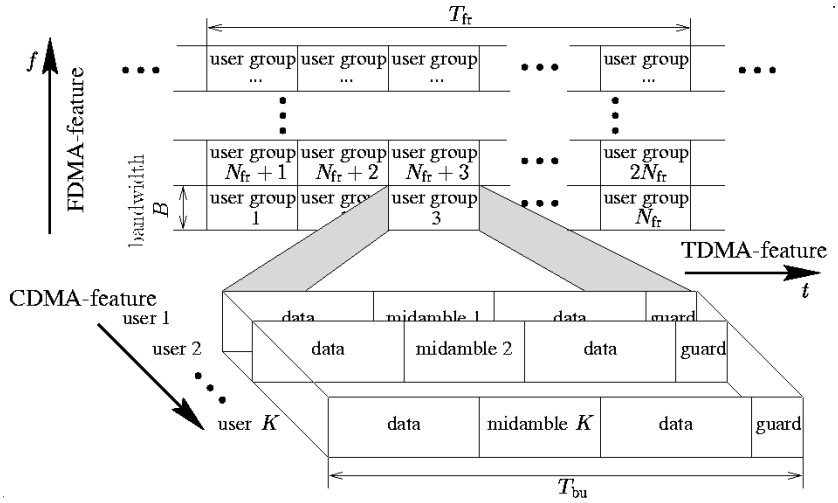

Fig. 1. Frame and burst structure for the considered TD-CDMA mobile radio system [8], [13].

mobile users are active, each using a user specific spreading code, which allows signal separation at the receiver. The frame structure of this time-slotted CDMA concept is illustrated in Fig. 1, where $B, T_{fr}, N_{fr}, T_{bu}$, and K denote the bandwidth of a frequency band, the duration of a TDMA frame, the number of bursts per TDMA frame, the burst duration, and the number of users per frequency band and time slot, respectively. A burst consists of two data blocks separated by a user specific midamble, which is used for a combined DOA and joint channel estimation, and a guard interval [see Fig. 1]. The adopted frame and burst structure are similar to that used in GSM and thus beneficially facilitates backward compatibility with this *de facto* world standard as well as with the adoption of a GSM-based multiple-access scheme.

The paper is organized as follows. In Section II, the system model for the channel estimation process is described when multiantenna array configurations are employed at the uplink receiver. Section III deals with the noise correlation properties, which can be exploited for enhancing the channel estimation and the joint data detection. In Section IV, the combined DOA and joint channel estimation is described. Based on a new mathematical representation of the joint data detection problem, the system model and a novel joint data detection technique, taking into account the estimated DOA's and the associated channel impulse responses, are presented in Section V. Simulation results are presented and discussed in Section VI. Section VII summarizes the basic results and concludes the paper.

In the present paper, complex quantities are underlined, and vectors and matrices are in bold face. Furthermore, the symbols $(\cdot)^*$, $(\cdot)^T$, and $E\{\cdot\}$ designate the complex conjugation, transposition, and expectation, respectively.

II. System Model for the Channel Estimation

In the following, a time discrete system model for the purpose of the channel estimation in the equivalent low-pass domain is considered. It is assumed that burst synchronization is achieved by using particular access and synchronization bursts as it is, e.g., the case in GSM [14]. Multiantenna array configurations

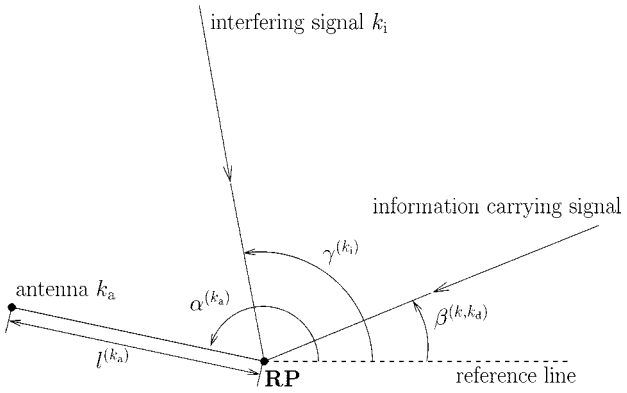

Fig. 2. For the definition of multiantenna configuration parameters.

are assumed to be used at the receiver. The following numbering scheme is adopted:

K	total number of users active in the same frequency band and time slot;
$k = 1 \cdots K$	consecutive user number;
$K_d^{(k)}$	total number of DOA's of signals from transmitter k;
$k_d = 1 \cdots K_d^{(k)}$	consecutive number of DOA of signals from transmitter k;
K_a	total number of array elements;
$k_a = 1 \cdots K_a$	consecutive number of array element;
K_i	total number of interfering signals;
$k_i = 1 \cdots K_i$	consecutive number of interfering signal.

The definition of further quantities is illustrated in Fig. 2. The k_dth DOA of a signal coming from transmitter k is denoted by $\beta^{(k,k_d)}$ and the DOA of the k_ith interfering signal is denoted by $\gamma^{(k_i)}$. The k_ath array element has a distance of $l^{(k_a)}$ to an assumed reference point (RP) and the angle spanned by the reference line and the line connecting the referred array element with the RP is termed $\alpha^{(k_a)}$.

For each DOA of a desired signal one channel impulse response can be defined which could be observed by an omnidirectional antenna located at the RP [3], [15]. The channel impulse response vector for the k_dth DOA of the kth user will be

denoted as $\underline{\boldsymbol{h}}_d^{(k,\,k_d)}$ and has length W [16], which can incorporate large delay spreads. The subscript d indicates that we refer to channels that depend on the DOA's of each user. We will refer to these channels as the directional ones, in order to distinguish from the channels that are not connected with DOA's (see also [3]). With the user specific $W \times K_d^{(k)}$ matrices

$$\underline{\boldsymbol{H}}_d^{(k)} = \left[\underline{\boldsymbol{h}}_d^{(k,\,1)}, \underline{\boldsymbol{h}}_d^{(k,\,2)} \cdots \underline{\boldsymbol{h}}_d^{(k,\,K_d^{(k)})}\right], \qquad k = 1 \cdots K \quad (1)$$

the directional channel impulse response vectors from all users can be combined to the $W \times K_d$ matrix

$$\underline{\boldsymbol{H}}_d = \left[\underline{\boldsymbol{H}}_d^{(1)}, \underline{\boldsymbol{H}}_d^{(2)} \cdots \underline{\boldsymbol{H}}_d^{(K)}\right] \quad (2)$$

where

$$K_d = \sum_{k=1}^{K} K_d^{(k)}. \quad (3)$$

Accordingly, the channel impulse response vectors corresponding to the links between the kth user and every array element k_a, $k_a = 1 \cdots K_a$, are combined to the $W \times K_a$ matrix

$$\underline{\boldsymbol{H}}^{(k)} = \left[\underline{\boldsymbol{h}}^{(k,\,1)}, \underline{\boldsymbol{h}}^{(k,\,2)} \cdots \underline{\boldsymbol{h}}^{(k,\,K_a)}\right] \quad (4)$$

and the channel impulse responses from all users are then arranged to the $KW \times K_a$ matrix

$$\underline{\boldsymbol{H}} = \left[\underline{\boldsymbol{H}}^{(1)T}, \underline{\boldsymbol{H}}^{(2)T} \cdots \underline{\boldsymbol{H}}^{(K)T}\right]^T. \quad (5)$$

The signals are assumed to be narrowband, i.e., their amplitudes and phases vary slowly with respect to the propagation time across the array. Then, the propagation delay can be modeled by multiplying the signal complex envelope by a complex exponential [17], the phase factor $e^{j\psi(k,\,k_a,\,k_d)}$, where

$$\psi(k,\,k_a,\,k_d) = 2\pi\,\frac{l^{(k_a)}}{\lambda}\,\cos\left(\beta^{(k,\,k_d)} - \alpha^{(k_a)}\right) \quad (6)$$

$k = 1 \cdots K$, $k_a = 1 \cdots K_a$, and $k_d = 1 \cdots K_d^{(k)}$ are the spatial frequencies with respect to the RP and λ denotes the carrier wavelength. In this case, the channel impulse response vector $\underline{\boldsymbol{h}}^{(k,\,k_a)}$ is related to the directional channel impulse responses $\underline{\boldsymbol{h}}_d^{(k,\,k_d)}$, $k_d = 1 \cdots K_d^{(k)}$, corresponding to the different DOA's of the kth user by

$$\underline{\boldsymbol{h}}^{(k,\,k_a)} = \sum_{k_d=1}^{K_d^{(k)}} e^{j\psi(k,\,k_a,\,k_d)} \cdot \underline{\boldsymbol{h}}_d^{(k,\,k_d)}. \quad (7)$$

With

$$\underline{\boldsymbol{A}}^{(k)} = \left[\underline{\boldsymbol{a}}^{(k,\,1)}, \underline{\boldsymbol{a}}^{(k,\,2)} \cdots \underline{\boldsymbol{a}}^{(k,\,K_d^{(k)})}\right], \qquad k = 1 \cdots K \quad (8)$$

the $K_a \times K_d^{(k)}$ user specific steering matrix [17], [18] and (7), the relation between the combined channel impulse responses for the kth user contained in the matrix $\underline{\boldsymbol{H}}^{(k)}$ [see (4)] and the directional channel impulse responses for the kth user contained in the matrix $\underline{\boldsymbol{H}}_d^{(k)}$ [see (1)] is given by

$$\underline{\boldsymbol{H}}^{(k)} = \sum_{k_d=1}^{K_d^{(k)}} \underline{\boldsymbol{h}}_d^{(k,\,k_d)} \underline{\boldsymbol{a}}^{(k,\,k_d)T} = \underline{\boldsymbol{H}}_d^{(k)} \underline{\boldsymbol{A}}^{(k)T}. \quad (9)$$

Let now $\underline{\boldsymbol{G}}^{(k)}$, $k = 1 \cdots K$, be the $L \times W$ Toeplitz matrix of the midamble training sequence for the kth user [16]. Here, L is the number of the samples of the received signal that depend exclusively on the midamble training sequence and not on the transmitted data [16]. The matrix $\underline{\boldsymbol{G}}$ of the user specific midamble training sequences, known at the receiver, which will be used for the process of the joint channel estimation, is given by [16]

$$\underline{\boldsymbol{G}} = \left[\underline{\boldsymbol{G}}^{(1)}, \underline{\boldsymbol{G}}^{(2)} \cdots \underline{\boldsymbol{G}}^{(K)}\right]. \quad (10)$$

The part of the received signal for each array element which depends exclusively on the midamble training sequences is denoted by $\underline{\boldsymbol{e}}_m^{(k_a)}$, $k_a = 1 \cdots K_a$, and these K_a vectors are arranged columnwise in the $L \times K_a$ matrix $\underline{\boldsymbol{E}}_m$. If we further admit additive noise $\underline{\boldsymbol{n}}_m^{(k_a)}$, $k_a = 1 \cdots K_a$, at each array element and arrange the K_a noise vectors in the $L \times K_a$ matrix $\underline{\boldsymbol{N}}_m$, the following equation relates the received signals at the K_a array elements, which depend exclusively on the midamble training sequences, to the channel impulse responses from all K users:

$$\underline{\boldsymbol{E}}_m = \underline{\boldsymbol{G}} \cdot \underline{\boldsymbol{H}} + \underline{\boldsymbol{N}}_m. \quad (11)$$

Furthermore, inserting (5), (9), and (10) into (11) yields

$$\begin{aligned}\underline{\boldsymbol{E}}_m &= \left[\underline{\boldsymbol{G}}^{(1)}, \underline{\boldsymbol{G}}^{(2)} \cdots \underline{\boldsymbol{G}}^{(K)}\right] \\ &\quad \cdot \left[\underline{\boldsymbol{A}}^{(1)} \underline{\boldsymbol{H}}_d^{(1)T}, \underline{\boldsymbol{A}}^{(2)} \underline{\boldsymbol{H}}_d^{(2)T} \cdots \underline{\boldsymbol{A}}^{(K)} \underline{\boldsymbol{H}}_d^{(K)T}\right]^T + \underline{\boldsymbol{N}}_m \\ &= \sum_{k=1}^{K} \underline{\boldsymbol{G}}^{(k)} \underline{\boldsymbol{H}}_d^{(k)} \underline{\boldsymbol{A}}^{(k)T} + \underline{\boldsymbol{N}}_m. \end{aligned} \quad (12)$$

Moreover, we define

$$\underline{\boldsymbol{e}}_m = \mathrm{vec}\{\underline{\boldsymbol{E}}_m\} \quad (13)$$

$$\underline{\boldsymbol{h}} = \mathrm{vec}\{\underline{\boldsymbol{H}}\} \quad (14)$$

$$\underline{\boldsymbol{h}}_d = \mathrm{vec}\{\underline{\boldsymbol{H}}_d\} \quad (15)$$

$$\underline{\boldsymbol{n}}_m = \mathrm{vec}\{\underline{\boldsymbol{N}}_m\} \quad (16)$$

where the $\mathrm{vec}\{\cdot\}$-operator denotes a vector-valued function that maps an $m \times n$ matrix into an mn-dimensional column vector by stacking the columns of the matrix [19]. According to these definitions, by using the property which combines the Kronecker

product with the vec$\{\cdot\}$-operator [19], (11) and (12) can be written, respectively, in the following simple forms:

$$\underline{\boldsymbol{e}}_m = \left(\boldsymbol{I}^{(K_a)} \otimes \underline{\boldsymbol{G}}\right) \cdot \underline{\boldsymbol{h}} + \underline{\boldsymbol{n}}_m \tag{17}$$

$$\underline{\boldsymbol{e}}_m = \underline{\boldsymbol{G}}_d \underline{\boldsymbol{h}}_d + \underline{\boldsymbol{n}}_m \tag{18}$$

where the symbol $\otimes$ denotes the Kronecker product, $\boldsymbol{I}^{(K_a)}$ is the $K_a \times K_a$ identity matrix, and

$$\underline{\boldsymbol{G}}_d = \left[\underline{\boldsymbol{A}}^{(1)} \otimes \underline{\boldsymbol{G}}^{(1)}, \underline{\boldsymbol{A}}^{(2)} \otimes \underline{\boldsymbol{G}}^{(2)} \cdots \underline{\boldsymbol{A}}^{(K)} \otimes \underline{\boldsymbol{G}}^{(K)}\right] \tag{19}$$

[see also (8) and (10)]. The representations (17) and (18) of the combined received signal at all K_a array elements that depends exclusively on the midamble training sequences will be used for the combined DOA and joint channel estimation to be presented in Section IV. Before this, the correlation properties of the interfering signals in the case of multiantenna arrays will be discussed.

III. Correlation Properties of the Noise

In digital cellular mobile radio systems, the reliability and the transmission quality is determined by the multiple-access interference. Therefore, digital cellular mobile radio systems are often characterized as interference limited systems [20], [21]. The level of the multiple-access interference depends on, among other parameters, the multiple-access scheme and the detection principle. In TD-CDMA mobile radio systems, the intracell interference, i.e., the interference from users assigned to the considered BS, is eliminated by the joint detection algorithm employed at the receiver [7]. Consequently, the intercell interference, i.e., the interference from users of other cells, plays the most important role on the transmission quality and the reliability of the system. Since we refer to a cellular system, the user signals possess the same spectral properties, which are determined by the modulation scheme, as well as the transmitter and receiver filters. Furthermore, the directional inhomogeneity of the mobile radio channel introduces at the considered BS directional intercell noise components, i.e., noise signals with certain DOA's, which also have a certain impinging power. This information for the intercell interference can be used at the receiver in order to enhance its performance [22]. In the sequel, we will discuss the noise properties for the channel estimation procedure. The same analysis is also applicable to the data detection process, as shown at the end of the present section.

It is assumed there are K_i interfering signals present. If the k_ith interfering signal at the RP is expressed as the vector $\underline{\boldsymbol{n}}_d^{(k_i)}$ [16] of length L, the phase factor for the k_ith interferer at the k_ath array element is given by

$$\phi(k_i, k_a) = 2\pi \frac{l^{(k_a)}}{\lambda} \cos\left(\gamma^{(k_i)} - \alpha^{(k_a)}\right) \tag{20}$$

see also (6) and Fig. 2. Therefore, the total noise vector at the k_ath array element is related to the noise vectors $\underline{\boldsymbol{n}}_d^{(k_i)}$, $k_i = 1 \cdots K_i$, via

$$\underline{\boldsymbol{n}}_m^{(k_a)} = \sum_{k_i=1}^{K_i} e^{j\phi(k_i, k_a)} \cdot \underline{\boldsymbol{n}}_d^{(k_i)}. \tag{21}$$

Let now

$$\underline{\boldsymbol{R}}_m^{(i,j)} = E\left\{\underline{\boldsymbol{n}}_m^{(i)} \underline{\boldsymbol{n}}_m^{(j)*T}\right\}, \qquad i, j = 1 \cdots K_a \tag{22}$$

denote the $L \times L$ covariance matrix of the noise vectors $\underline{\boldsymbol{n}}_m^{(i)}$ of the ith array element and $\underline{\boldsymbol{n}}_m^{(j)}$ of the jth array element. Then, the covariance matrix of the combined noise vector from all K_a antenna elements is the $LK_a \times LK_a$ matrix

$$\underline{\boldsymbol{R}}_m = E\left\{\underline{\boldsymbol{n}}_m \underline{\boldsymbol{n}}_m^{*T}\right\} \tag{23}$$

with its (i, j)th block equal to $\underline{\boldsymbol{R}}_m^{(i,j)}$ of (22).

Furthermore, it is assumed that the noise signals are pairwise uncorrelated, i.e.,

$$E\left\{\underline{\boldsymbol{n}}_d^{(l)} \underline{\boldsymbol{n}}_d^{(m)*T}\right\} = 0, \qquad \text{for } l \neq m \tag{24}$$

and they have the same spectral form. If the noise power of the k_ith interferer is defined as

$$\left(\sigma^{(k_i)}\right)^2 = E\left\{\left|\underline{n}_{d,l}^{(k_i)}\right|^2\right\}, \qquad l = 1 \cdots L \tag{25}$$

the spectral form of the interfering signals is given by the $L \times L$ covariance matrix

$$\tilde{\underline{\boldsymbol{R}}}_m = \frac{1}{\left(\sigma^{(k_i)}\right)^2} E\left\{\underline{\boldsymbol{n}}_d^{(k_i)} \underline{\boldsymbol{n}}_d^{(k_i)*T}\right\}, \qquad k_i = 1 \cdots K_i. \tag{26}$$

Notice that $\tilde{\underline{\boldsymbol{R}}}_m$ is the same for all K_i interferers. Let us define the scalars

$$\begin{aligned} \underline{r}_{i,j} &= \underline{r}_{i,j}^* \\ &= \sum_{k_i=1}^{K_i} \left(\sigma^{(k_i)}\right)^2 e^{j(\phi^{(k_i,i)} - \phi^{(k_i,j)})}, \quad i, j = 1 \cdots K_a \end{aligned} \tag{27}$$

which depend on the noise powers and the phase factors of the interfering signals [see also (20)]. Then, the covariance matrix $\underline{\boldsymbol{R}}_m^{(i,j)}$, defined in (22), takes the form

$$\underline{\boldsymbol{R}}_m^{(i,j)} = E\left\{\underline{\boldsymbol{n}}_m^{(i)} \underline{\boldsymbol{n}}_m^{(j)*T}\right\} = \underline{r}_{i,j} \cdot \tilde{\underline{\boldsymbol{R}}}_m, \qquad i, j = 1 \cdots K_a \tag{28}$$

and the covariance matrix of the combined received noise vector [see (23)] is a $LK_a \times LK_a$ matrix with its (i, j)th block equal to $\underline{r}_{i,j} \cdot \tilde{\underline{\boldsymbol{R}}}_m$ of (28). If we define the $K_a \times K_a$ matrix $\underline{\boldsymbol{R}}_d$ with element (i, j) equal to $\underline{r}_{i,j}$ [see (27)], then the covariance matrix of the combined noise vector from all array elements takes the simple form [15]

$$\underline{\boldsymbol{R}}_m = \underline{\boldsymbol{R}}_d \otimes \tilde{\underline{\boldsymbol{R}}}_m. \tag{29}$$

The matrix $\underline{\boldsymbol{R}}_d$ depends exclusively on the DOA's and the noise powers of the K_i interferers and therefore is also valid for the data detection, which is considered in Section V. The covariance matrix $\tilde{\underline{\boldsymbol{R}}}_m$ contains information regarding the spectral form of the interfering signals, which is assumed to be identical for all interfering signals, an assumption which is justified by the fact that we refer to a cellular mobile radio system that uses signals with the same spectral properties. $\tilde{\underline{\boldsymbol{R}}}_m$ depends on the length of the part of the received signal which is used, i.e., for the channel

estimation it has dimensions $L \times L$, whereas for the data detection it has dimensions $(NQ+W-1)\times(NQ+W-1)$ and will be addressed as $\underline{\tilde{\boldsymbol{R}}}_n$. N is the number of transmitted symbols per user and Q the length of the user specific spreading sequence (see also the analysis of Section V). Therefore, the covariance matrix of the combined received vector from all array elements for the data detection is expressed as

$$\underline{\boldsymbol{R}}_n = \underline{\boldsymbol{R}}_d \otimes \underline{\tilde{\boldsymbol{R}}}_n. \tag{30}$$

IV. Combined DOA and Joint Channel Estimation

In this section, a novel approach to the channel estimation process for a TD-CDMA mobile radio system will be presented. This approach can be divided into three steps, which will be illustrated individually in this section.

- In a first step, the channel impulse responses for the links between each user and each array element are estimated according to [16], leading to the separation of the channel impulse responses which belong to the different users.
- Then, the user specific channel impulse responses are used for a user specific DOA estimation.
- In a third step, the information about the DOA's and the channel impulse responses of every user is exploited for an enhanced joint channel estimation, which leads to improved channel impulse response estimates.

It should be noted that the information carrying signals of a certain user should not have more discrete DOA's than the number of array elements employed at the BS receiver, i.e., it will be assumed there exist $K_d^{(k)} < K_a$, $k = 1 \cdots K$, discrete DOA's for the user k. Nevertheless, there are scenarios in mobile radio where the impinging signals are confined within a relative small range. This is a typical situation in urban propagation environments. In these cases, one dominant DOA from this range is used for the enhanced joint channel estimation, which means that even if $K_d^{(k)} > K_a, k = 1 \cdots K$, the novel scheme provides a way for taking advantage of the directional inhomogeneity of the mobile radio channel. In Section VI, simulation results will demonstrate the improvement by the new concept concerning, on the one hand, the channel impulse response estimates and, on the other hand, the link level performance of the considered TD-CDMA employing this approach for different scenarios in rural and urban propagation environments.

A. Conventional Joint Channel Estimation

According to (17) and (29), the maximum-likelihood estimate $\underline{\hat{\boldsymbol{h}}}$ of the combined channel impulse response vector $\underline{\boldsymbol{h}}$, defined in (14), is given by [3]

$$\underline{\hat{\boldsymbol{h}}} = \left(\boldsymbol{I}^{(K_a)} \otimes \underline{\boldsymbol{M}}_m\right) \underline{\boldsymbol{e}}_m \tag{31}$$

where

$$\underline{\boldsymbol{M}}_m = \left(\underline{\boldsymbol{G}}^{*T} \underline{\tilde{\boldsymbol{R}}}_m^{-1} \underline{\boldsymbol{G}}\right)^{-1} \underline{\boldsymbol{G}}^{*T} \underline{\tilde{\boldsymbol{R}}}_m^{-1}. \tag{32}$$

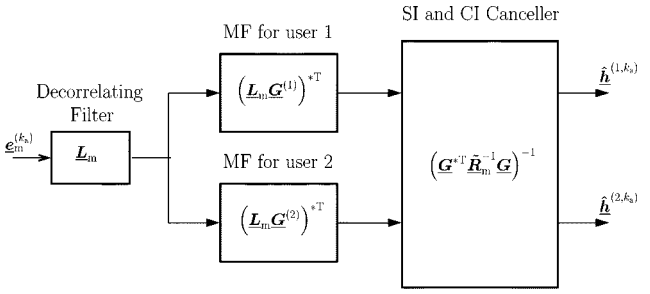

Fig. 3. Implementation of the conventional channel estimator at the k_ath array element for the case of $K = 2$ users.

Equation (31) shows that K_a individual joint channel estimation processes take place, each one exactly as it is described in [16]

$$\underline{\hat{\boldsymbol{h}}}^{(k_a)} = \left(\underline{\boldsymbol{G}}^{*T} \underline{\tilde{\boldsymbol{R}}}_m^{-1} \underline{\boldsymbol{G}}\right)^{-1} (\underline{\boldsymbol{L}}_m \underline{\boldsymbol{G}})^{*T} \underline{\boldsymbol{L}}_m \underline{\boldsymbol{e}}_m^{(k_a)}, \quad k_a = 1 \cdots K_a \tag{33}$$

where the Cholesky decomposition [23]

$$\underline{\tilde{\boldsymbol{R}}}_m^{-1} = \underline{\boldsymbol{L}}_m^{*T} \underline{\boldsymbol{L}}_m \tag{34}$$

has been used. The multiplication of the received signal at the k_ath array element by $\underline{\boldsymbol{L}}_m$ prewhitens or decorrelates the noise, whereas the term $(\underline{\boldsymbol{L}}_m \underline{\boldsymbol{G}}^{(k)})^{*T}$ indicates the operations of K matched filters to every user k, $k = 1 \cdots K$ [see also (10)]. Finally, the multiplication by $(\underline{\boldsymbol{G}}^{*T} \underline{\tilde{\boldsymbol{R}}}_m^{-1} \underline{\boldsymbol{G}})^{-1}$ in (33) cancels the effect of self-interference (SI) and cross interference (CI) [6], [27]. The above-mentioned operations are illustrated in Fig. 3 for the easy to survey case of $K = 2$ users and for the k_ath array element, $k_a = 1 \cdots K_a$. We will refer to this type of joint channel estimation and the associated joint data detection as the conventional scheme, in order to make the distinction from the combined DOA and joint channel estimation, presented in this section, and the corresponding joint data detection, presented in Section V, which will be addressed as the enhanced scheme.

B. DOA Estimation

Since the result of the process of the joint channel estimation is to produce separate estimates for the elements of the channel impulse response vectors $\underline{\boldsymbol{h}}^{(k_a)}$, $k_a = 1 \cdots K_a$ [see (33)] and consequently for the combined channel impulse response vector $\underline{\boldsymbol{h}}$ [see (14)], the parts of $\underline{\hat{\boldsymbol{h}}}$ that belong to the same user can be used for the purpose of a DOA estimation as described in the sequel.

Let $\underline{\hat{\boldsymbol{H}}}$ denote the matrix that contains the estimates of the channel impulse responses, arranged as in (5). Then, the estimate of the channel impulse response vector $\underline{\boldsymbol{h}}$ can be expressed as

$$\underline{\hat{\boldsymbol{h}}} = \mathrm{vec}\{\underline{\hat{\boldsymbol{H}}}\}. \tag{35}$$

According to (31) and (35), the matrix $\underline{\hat{\boldsymbol{H}}}$ can be written in its transposed form as

$$\underline{\hat{\boldsymbol{H}}}^T = \underline{\boldsymbol{H}}^T + \underline{\boldsymbol{N}}_m^T \underline{\boldsymbol{M}}_m^T \tag{36}$$

where $\underline{\boldsymbol{M}}_m$ is defined in (32). According to (5), we can use the blocks of $\underline{\boldsymbol{H}}$ that depend only on one user and perform a user

specific DOA estimation for every user k, $k = 1 \cdots K$. The extraction of the blocks $\underline{\boldsymbol{H}}^{(k)T}$, $k = 1 \cdots K$, can be described as

$$\underline{\boldsymbol{H}}^{(k)T} = \underline{\boldsymbol{H}}^{T} \left(\boldsymbol{u}^{(k)} \otimes \boldsymbol{I}^{(W)} \right) \tag{37}$$

where $\boldsymbol{u}^{(k)}$ is the $K \times 1$ identity column vector for the kth user, with its elements defined as

$$u_l^{(k)} = \begin{cases} l, & l = k \\ 0, & \text{otherwise} \end{cases} \tag{38}$$

and $\boldsymbol{I}^{(W)}$ is the $W \times W$ identity matrix. According to (37), we can obtain from (9) and (36)

$$\hat{\underline{\boldsymbol{H}}}^{(k)T} = \underline{\boldsymbol{A}}^{(k)} \underline{\boldsymbol{H}}_d^{(k)T} + \underline{\boldsymbol{N}}_m^T \underline{\boldsymbol{M}}_m^T \left(\boldsymbol{u}^{(k)} \otimes \boldsymbol{I}^{(W)} \right), \quad k = 1 \cdots K. \tag{39}$$

If we define

$$\underline{\boldsymbol{X}}^{(k)} = \hat{\underline{\boldsymbol{H}}}^{(k)T} \tag{40}$$

$$\underline{\boldsymbol{S}}^{(k)} = \underline{\boldsymbol{H}}_d^{(k)T} \tag{41}$$

$$\underline{\boldsymbol{N}}^{(k)} = \underline{\boldsymbol{N}}_m^T \underline{\boldsymbol{M}}_m^T \left(\boldsymbol{u}^{(k)} \otimes \boldsymbol{I}^{(W)} \right) \tag{42}$$

(39) can be written as

$$\underline{\boldsymbol{X}}^{(k)} = \underline{\boldsymbol{A}}^{(k)} \underline{\boldsymbol{S}}^{(k)} + \underline{\boldsymbol{N}}^{(k)}, \qquad k = 1 \cdots K \tag{43}$$

where $\underline{\boldsymbol{X}}^{(k)}$ denotes the noise-corrupted measurement matrix [24] of the kth user composed of W snapshots. $\underline{\boldsymbol{S}}^{(k)}$ and $\underline{\boldsymbol{N}}^{(k)}$ are the signal and noise matrices [24] of the kth user, respectively, and $\underline{\boldsymbol{A}}^{(k)}$ is the array steering matrix that depends on the DOA's of the user k [see (8)]. According to (43), K different DOA estimation processes can be performed. An algorithm that produces increased estimation accuracy with a reduced computational burden is one-dimensional (1-D) Unitary ESPRIT that can be applied to centro-symmetric array configurations [18]. This algorithm is used in the simulations for the estimation of the DOA's for every user.

C. Enhanced Joint Channel Estimation

Since the process of DOA estimation produces estimates for the DOA's of each user k, and consequently for the user specific array steering matrices $\underline{\boldsymbol{A}}^{(k)}$, $k = 1 \cdots K$ [see (8)], the maximum-likelihood estimate of the combined directional channel impulse response vector $\underline{\boldsymbol{h}}_d$ [see (15)] may be expressed as [23]

$$\hat{\underline{\boldsymbol{h}}}_d = \left(\underline{\boldsymbol{G}}_d^{*T} (\underline{\boldsymbol{R}}_d \otimes \tilde{\underline{\boldsymbol{R}}}_m)^{-1} \underline{\boldsymbol{G}}_d \right)^{-1} \underline{\boldsymbol{G}}_d^{*T} (\underline{\boldsymbol{R}}_d \otimes \tilde{\underline{\boldsymbol{R}}}_m)^{-1} \underline{\boldsymbol{e}}_m. \tag{44}$$

According to the definition of $\underline{\boldsymbol{G}}_d$ [see (19)], (44) can be written as

$$\hat{\underline{\boldsymbol{h}}}_d = \underline{\boldsymbol{X}}_m^{-1} \begin{bmatrix} \underline{\boldsymbol{A}}^{(1)*T} \otimes \underline{\boldsymbol{G}}^{(1)*T} \\ \vdots \\ \underline{\boldsymbol{A}}^{(K)*T} \otimes \underline{\boldsymbol{G}}^{(K)*T} \end{bmatrix} \left(\underline{\boldsymbol{R}}_d^{-1} \otimes \tilde{\underline{\boldsymbol{R}}}_m^{-1} \right) \underline{\boldsymbol{e}}_m \tag{45}$$

where $\underline{\boldsymbol{X}}_m$ is a $(K_d W) \times (K_d W)$ matrix [see (3)], with its (l, m)th block of dimension $(K_d^{(l)} W) \times (K_d^{(m)} W)$ defined as

$$\underline{\boldsymbol{X}}_m^{(l,m)} = \left(\underline{\boldsymbol{A}}^{(l)*T} \underline{\boldsymbol{R}}_d^{-1} \underline{\boldsymbol{A}}^{(m)} \right) \otimes \left(\underline{\boldsymbol{G}}^{(l)*T} \tilde{\underline{\boldsymbol{R}}}_m^{-1} \underline{\boldsymbol{G}}^{(m)} \right) \tag{46}$$

$l = 1 \cdots K$, $m = 1 \cdots K$. Recall that the dimensions of the matrices $\underline{\boldsymbol{A}}^{(k)}$, $k = 1 \cdots K$, are $K_a \times K_d^{(k)}$, the dimension of $\underline{\boldsymbol{G}}^{(k)}$, $k = 1 \cdots K$, is $L \times W$, and the covariance matrices $\underline{\boldsymbol{R}}_d^{-1}$ and $\tilde{\underline{\boldsymbol{R}}}_m^{-1}$ are of dimensions $K_a \times K_a$ and $L \times L$, respectively. By using the definition for the combined received signal $\underline{\boldsymbol{e}}_m$ at all K_a array elements [see (13)], the definition for the matrix $\underline{\boldsymbol{X}}_m$ [see (46)] and properties of the Kronecker product [19], the estimate of the combined directional channel impulse response vector $\underline{\boldsymbol{h}}_d$ [see (44)], can be formulated as follows:

$$\hat{\underline{\boldsymbol{h}}}_d = \underline{\boldsymbol{X}}_m^{-1} \begin{bmatrix} \operatorname{vec} \left\{ \underline{\boldsymbol{G}}^{(1)*T} \tilde{\underline{\boldsymbol{R}}}_m^{-1} \underline{\boldsymbol{E}}_m \left(\underline{\boldsymbol{R}}_d^{-1} \right)^* \underline{\boldsymbol{A}}^{(1)*} \right\} \\ \operatorname{vec} \left\{ \underline{\boldsymbol{G}}^{(2)*T} \tilde{\underline{\boldsymbol{R}}}_m^{-1} \underline{\boldsymbol{E}}_m \left(\underline{\boldsymbol{R}}_d^{-1} \right)^* \underline{\boldsymbol{A}}^{(2)*} \right\} \\ \vdots \\ \operatorname{vec} \left\{ \underline{\boldsymbol{G}}^{(K)*T} \tilde{\underline{\boldsymbol{R}}}_m^{-1} \underline{\boldsymbol{E}}_m \left(\underline{\boldsymbol{R}}_d^{-1} \right)^* \underline{\boldsymbol{A}}^{(K)*} \right\} \end{bmatrix}. \tag{47}$$

Recalling the definition of $\underline{\boldsymbol{A}}^{(k)}$, $k = 1 \cdots K$ [see (8)], we introduce the following definitions for $k = 1 \cdots K$, $k_d = 1 \cdots K_d^{(k)}$:

$$\underline{\boldsymbol{M}}_{\mathrm{DMF},m}^{(k)} = \underline{\boldsymbol{G}}^{(k)*T} \tilde{\underline{\boldsymbol{R}}}_m^{-1} \tag{48}$$

$$\underline{\boldsymbol{w}}^{(k,k_d)} = \left(\underline{\boldsymbol{R}}_d^{-1} \right)^* \underline{\boldsymbol{a}}^{(k,k_d)*} \tag{49}$$

$$\underline{\boldsymbol{y}}_m^{(k,k_d)} = \underline{\boldsymbol{E}}_m \underline{\boldsymbol{w}}^{(k,k_d)}. \tag{50}$$

Following the same reasoning as in [6], $\underline{\boldsymbol{M}}_{\mathrm{DMF},m}^{(k)}$ can be considered as a decorrelating matched filter (DMF) for user k. $\underline{\boldsymbol{y}}_m^{(k,k_d)}$ denotes a beamformer (BF) which maximizes at its output the signal-to-noise ratio (SNR) [25] and has weighting factors $\underline{w}_{k_a}^{(k,k_d)}$, $k_a = 1 \cdots K_a$. In this case, (47) takes the form

$$\hat{\underline{\boldsymbol{h}}}_d = \underline{\boldsymbol{X}}_m^{-1} \left[\underline{\boldsymbol{b}}^{(1,1)T} \cdots \underline{\boldsymbol{b}}^{(1,K_d^{(1)})T} \bullet\bullet\bullet \underline{\boldsymbol{b}}^{(K,1)T} \cdots \underline{\boldsymbol{b}}^{(1,K_d^{(K)})T} \right]^T \tag{51}$$

where

$$\underline{\boldsymbol{b}}^{(k,k_d)} = \underline{\boldsymbol{M}}_{\mathrm{DMF},m}^{(k)} \underline{\boldsymbol{y}}_m^{(k,k_d)}, \qquad k = 1 \cdots K, \; k_d = 1 \cdots K_d. \tag{52}$$

The combination of the BF for the user k and its k_dth DOA with the decorrelating matched filter for user k [see (52)] can be described as a spatial decorrelating matched filter (SDMF). Finally, the multiplication by $\underline{\boldsymbol{X}}_m^{-1}$ in (51) cancels the effect of SI and CI [27]. The realization of this enhanced joint channel estimator is illustrated in Fig. 4 for the case of

$$K_a = 3, \quad K = 2, \quad K_d^{(1)} = 2, \quad K_d^{(2)} = 1. \tag{53}$$

The process of the combined DOA and joint channel estimation described in this section produces estimates for the channel impulse responses $\underline{\boldsymbol{h}}_d^{(k,k_d)}$, $k = 1 \cdots K$, $k_d = 1 \cdots K_d^{(k)}$ [see (15) and (51)] and their corresponding DOA's [see (8)]. This information enables in conjunction with the knowledge of the user specific CDMA codes the data detection according to the joint detection principle [7], [22]. The formulation of the joint detector which uses the additional information associated with the directional inhomogeneity of the mobile radio channel, i.e., the directional channel impulse responses and the corresponding DOA's are presented in the following section.

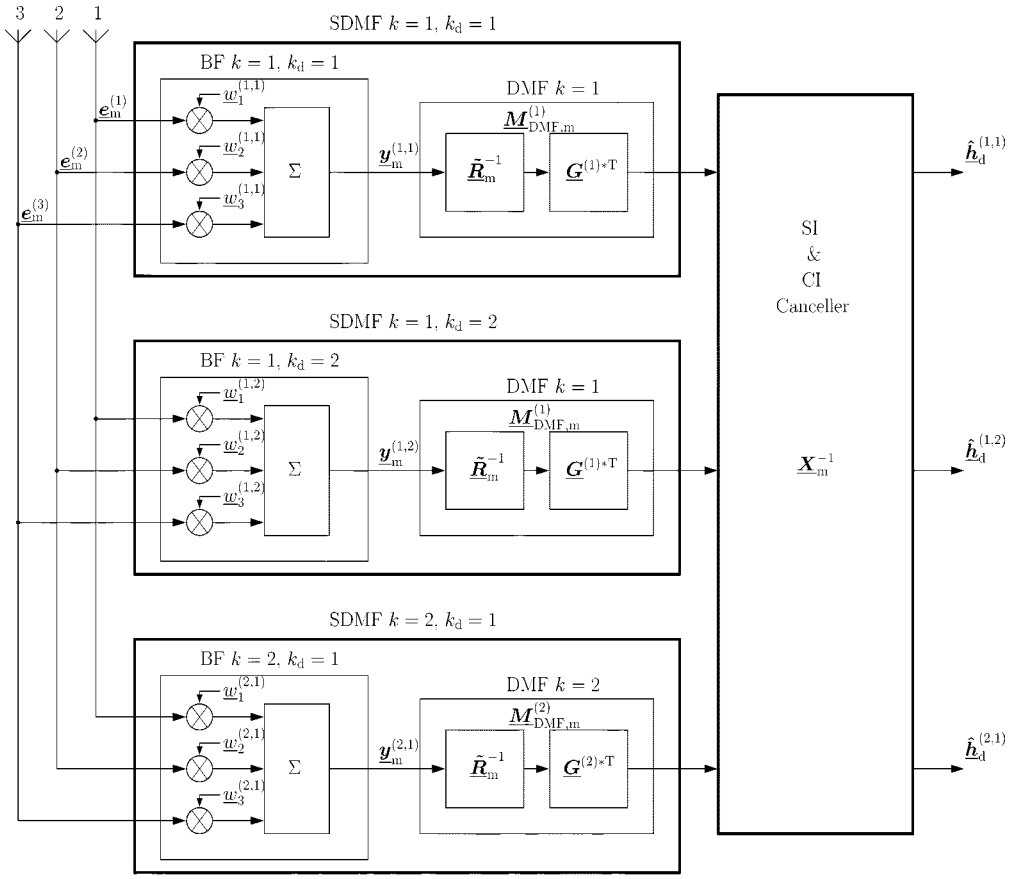

Fig. 4. Implementation of the enhanced channel estimator for the case of $K = 2$ users and $K_a = 3$ array elements.

V. Joint Data Detection

In this section, a novel technique for the joint detection of the data of all users assigned to the considered BS in a TD-CDMA mobile radio system is presented. This technique, which can be considered as an extension of the known ZF-BLE presented in [6]–[8], explicitly takes into account the DOA's of signals carrying information and the associated directional channel impulse responses, as these are produced from the combined DOA and joint channel estimation of Section IV. First, the discrete time low-pass representation of the uplink in a synchronous TD-CDMA mobile radio system will be described and then the novel joint data detection will be illustrated.

It is assumed the K users which are active in the same frequency band and time slot (see Fig. 1) transmit the complex data symbols $\underline{d}_n^{(k)}$, $n = 1 \cdots N$, $k = 1 \cdots K$, with rate $1/T_s$. The data symbols that pertain to one user are held in the vector $\underline{\boldsymbol{d}}^{(k)}$ of length N, and the data symbols of all K users can be combined to the vector [7], [8]

$$\underline{\boldsymbol{d}} = \left[\underline{\boldsymbol{d}}^{(1)T}, \underline{\boldsymbol{d}}^{(2)T} \cdots \underline{\boldsymbol{d}}^{(K)T}\right]^T \tag{54}$$

of length KN. The actual data rate may be varied according to the service provided or the desired transmission quality [6]. Each of the data symbols is spread by using the user specific signature sequences $\underline{\boldsymbol{c}}^{(k)}$, $k = 1 \cdots K$, of length Q at the transmitters to allow a coexistence of K active users in the same frequency band and time slot. The $\tilde{m}$-ary complex signature elements $\underline{c}_q^{(k)}$, $q = 1 \cdots Q$, are termed chips and are taken from the complex set

$$\underline{V}_c = \{\underline{v}_{c,1}, \underline{v}_{c,2} \cdots \underline{v}_{c,\tilde{m}}\}. \tag{55}$$

Depending on the set $\underline{V}_c$, different kinds of spectral spreading as, e.g., direct sequence CDMA or multicarrier CDMA can be realized [26]. The chip duration is given by

$$T_c = \frac{T_s}{Q}. \tag{56}$$

With the K user specific $NQ \times N$ matrices

$$\underline{\boldsymbol{C}}^{(k)} = \boldsymbol{I}^{(N)} \otimes \underline{\boldsymbol{c}}^{(k)}, \qquad k = 1 \cdots K \tag{57}$$

which describe the spectral spreading operation of the data symbols $\underline{d}_n^{(k)}$ of user k, we can form the block-diagonal matrix

$$\underline{\boldsymbol{C}} = \text{blockdiag}\left[\underline{\boldsymbol{C}}^{(1)}, \underline{\boldsymbol{C}}^{(2)} \cdots \underline{\boldsymbol{C}}^{(K)}\right] \tag{58}$$

which contains the signature sequences of all K users. With the directional channel impulse response vectors $\underline{\boldsymbol{h}}_d^{(k,k_d)}$ [see (1), (2), and (15)], we form the matrices $\underline{\boldsymbol{H}}_{da}^{(k,k_d)}$, $k = 1 \cdots K$, $k_d = 1 \cdots K_d$, with elements

$$\left[\underline{\boldsymbol{H}}_{da}^{(k,k_d)}\right]_{n+w-1,\,n} = \begin{cases} \underline{h}_{d,\,w}^{(k,k_d)}, & w = 1 \cdots W,\ n = 1 \cdots NQ \\ 0, & \text{otherwise.} \end{cases} \tag{59}$$

Using the $K_d^{(k)}(NQ+W-1)\times NQ$ matrix

$$\underline{\boldsymbol{H}}_{da}^{(k)} = \left[\underline{\boldsymbol{H}}_{da}^{(k,1)T}, \underline{\boldsymbol{H}}_{da}^{(k,2)T} \cdots \underline{\boldsymbol{H}}_{da}^{(k,K_d^{(k)})T}\right]^T, \quad k = 1\cdots K \tag{60}$$

which contains the directional channel impulse responses that correspond to the kth user, we define the block diagonal matrix

$$\underline{\boldsymbol{H}}_{da} = \text{blockdiag}\left[\underline{\boldsymbol{H}}_{da}^{(1)}, \underline{\boldsymbol{H}}_{da}^{(2)} \cdots \underline{\boldsymbol{H}}_{da}^{(K)}\right] \tag{61}$$

which contains the directional channel impulse responses for each user and each DOA. Furthermore, the array steering matrices $\underline{\boldsymbol{A}}^{(k)}$ [see (8)] can be combined to the matrix

$$\underline{\boldsymbol{A}} = \left[\underline{\boldsymbol{A}}^{(1)}, \underline{\boldsymbol{A}}^{(2)} \cdots \underline{\boldsymbol{A}}^{(K)}\right] \tag{62}$$

and the following definition is introduced:

$$\underline{\boldsymbol{A}}_d\underline{\boldsymbol{A}} \otimes \boldsymbol{I}^{(NQ+W-1)}. \tag{63}$$

The transmitted signals are received at the BS over K_a array elements. The received signal at the k_ath array element, which depends exclusively on the transmitted data symbols and not on the midamble training sequences, is denoted by $\underline{\boldsymbol{e}}^{(k_a)}$, $k_a = 1\cdots K_a$, and has length $NQ+W-1$ [6]. These K_a vectors can be arranged in the $(NQ+W-1)\times K_a$ matrix

$$\underline{\boldsymbol{E}} = \left[\underline{\boldsymbol{e}}^{(1)}, \underline{\boldsymbol{e}}^{(2)} \cdots \underline{\boldsymbol{e}}^{(K_a)}\right]. \tag{64}$$

With (64) and the $\text{vec}\{\cdot\}$-operator [19], the combined received signal at all K_a antennas which depends exclusively on the transmitted data symbols of all K users can be expressed as

$$\underline{\boldsymbol{e}} = \text{vec}\{\underline{\boldsymbol{E}}\}. \tag{65}$$

We further admit additive noise at each array element in the form of the vectors $\underline{\boldsymbol{n}}^{(k_a)}$, $k_a = 1\cdots K_a$, and we arrange these K_a vectors in the combined noise vector

$$\underline{\boldsymbol{n}} = \left[\underline{\boldsymbol{n}}^{(1)T}, \underline{\boldsymbol{n}}^{(2)T} \cdots \underline{\boldsymbol{n}}^{(K_a)T}\right]^T \tag{66}$$

of length $K_a(NQ+W-1)$. Then, according to (58), (61), and (63), the combined received signal $\underline{\boldsymbol{e}}$ of (65) can be expressed as

$$\underline{\boldsymbol{e}} = \underline{\boldsymbol{A}}_d\underline{\boldsymbol{H}}_{da}\underline{\boldsymbol{C}}\,\underline{\boldsymbol{d}} + \underline{\boldsymbol{n}} \tag{67}$$

(see also [3]).

According to (30) and (67), the estimate $\hat{\underline{\boldsymbol{d}}}$ of the combined data vector $\underline{\boldsymbol{d}}$ [see (54)] based on the ZF-BLE can be expressed as

$$\hat{\underline{\boldsymbol{d}}} = \left(\underline{\boldsymbol{C}}^{*T}\underline{\boldsymbol{H}}_{da}^{*T}\underline{\boldsymbol{A}}_d^{*T}\left(\underline{\boldsymbol{R}}_d^{-1}\otimes\tilde{\underline{\boldsymbol{R}}}_n^{-1}\right)\underline{\boldsymbol{A}}_d\underline{\boldsymbol{H}}_{da}\underline{\boldsymbol{C}}\right)^{-1} \cdot \underline{\boldsymbol{C}}^{*T}\underline{\boldsymbol{H}}_{da}^{*T}\underline{\boldsymbol{A}}_d^{*T}\left(\underline{\boldsymbol{R}}_d^{-1}\otimes\tilde{\underline{\boldsymbol{R}}}_n^{-1}\right)\underline{\boldsymbol{e}}. \tag{68}$$

Introducing the definition

$$\underline{\boldsymbol{X}} = \left(\underline{\boldsymbol{C}}^{*T}\underline{\boldsymbol{H}}_{da}^{*T}\underline{\boldsymbol{A}}_d^{*T}\left(\underline{\boldsymbol{R}}_d^{-1}\otimes\tilde{\underline{\boldsymbol{R}}}_n^{-1}\right)\underline{\boldsymbol{A}}_d\underline{\boldsymbol{H}}_{da}\underline{\boldsymbol{C}}\right)^{-1} \tag{69}$$

and applying (63), (69), and properties of the Kronecker product [19], (68) takes the form

$$\begin{aligned}\hat{\underline{\boldsymbol{d}}} &= \underline{\boldsymbol{X}}\,\underline{\boldsymbol{C}}^{*T}\underline{\boldsymbol{H}}_{da}^{*T}\left(\underline{\boldsymbol{A}}^{*T}\underline{\boldsymbol{R}}_d^{-1}\otimes\tilde{\underline{\boldsymbol{R}}}_n^{-1}\right)\text{vec}\{\underline{\boldsymbol{E}}\}\\ &= \underline{\boldsymbol{X}}\,\underline{\boldsymbol{C}}^{*T}\underline{\boldsymbol{H}}_{da}^{*T}\,\text{vec}\left\{\tilde{\underline{\boldsymbol{R}}}_n^{-1}\underline{\boldsymbol{E}}\left(\underline{\boldsymbol{R}}_d^{-1}\right)^T\underline{\boldsymbol{A}}^*\right\}\end{aligned} \tag{70}$$

where $\underline{\boldsymbol{E}}$ is defined in (64). Using the weighting vector $\underline{\boldsymbol{w}}^{(k,k_d)}$ of (49) and

$$\underline{\boldsymbol{y}}^{(k,k_d)} = \underline{\boldsymbol{E}}\,\underline{\boldsymbol{w}}^{(k,k_d)} \tag{71}$$

which describes a BF that maximizes the SNR at its output [25], (70) can be written as

$$\hat{\underline{\boldsymbol{d}}} = \underline{\boldsymbol{X}}\,\underline{\boldsymbol{C}}^{*T}\underline{\boldsymbol{H}}_{da}^{*T}\left(\boldsymbol{I}^{(K_d)}\otimes\tilde{\underline{\boldsymbol{R}}}_n^{-1}\right) \tag{72}$$

$$\cdot\left[\underline{\boldsymbol{y}}^{(1,1)T} \cdots \underline{\boldsymbol{y}}^{(1,K_d^{(1)})T} \bullet\bullet\bullet \underline{\boldsymbol{y}}^{(K,1)T} \cdots \underline{\boldsymbol{y}}^{(K,K_d^{(K)})T}\right]^T. \tag{73}$$

If we further define

$$\underline{\boldsymbol{Y}} = \underline{\boldsymbol{C}}^{*T}\underline{\boldsymbol{H}}_{da}^{*T}\left(\boldsymbol{I}^{(K_d)}\otimes\tilde{\underline{\boldsymbol{R}}}_n^{-1}\right) \tag{74}$$

the use of (58), the Cholesky decomposition [23]

$$\tilde{\underline{\boldsymbol{R}}}_n^{-1} = \underline{\boldsymbol{L}}_n^{*T}\underline{\boldsymbol{L}}_n \tag{75}$$

as well as the following definition:

$$\begin{aligned}\underline{\boldsymbol{Y}}^{(k)} &= \underline{\boldsymbol{C}}^{(k)*T}\underline{\boldsymbol{H}}_{da}^{(k)*T}\left(\boldsymbol{I}^{(K_d^{(k)})}\otimes\tilde{\underline{\boldsymbol{R}}}_n^{-1}\right)\\ &= \left[\left(\underline{\boldsymbol{L}}_n\underline{\boldsymbol{H}}_{da}^{(k,1)}\underline{\boldsymbol{C}}^{(k)}\right)^{*T}\underline{\boldsymbol{L}}_n \cdots \left(\underline{\boldsymbol{L}}_n\underline{\boldsymbol{H}}_{da}^{(k,K_d^{(k)})}\underline{\boldsymbol{C}}^{(k)}\right)^{*T}\underline{\boldsymbol{L}}_n\right],\\ &\quad k = 1\cdots K\end{aligned} \tag{76}$$

enable us to express $\underline{\boldsymbol{Y}}$ of (74) the following block-diagonal matrix:

$$\underline{\boldsymbol{Y}} = \text{blockdiag}\left[\underline{\boldsymbol{Y}}^{(1)}, \underline{\boldsymbol{Y}}^{(2)} \cdots \underline{\boldsymbol{Y}}^{(K)}\right]. \tag{77}$$

The diagonal blocks $\underline{\boldsymbol{Y}}^{(k)}$, $k = 1\cdots K$, are in general not of the same dimensions, since they depend on the number of DOA's associated with each user and denote the operations of DMF's [6] for user k and its DOA's $\beta^{(k,k_d)}$, $k_d = 1\cdots K_d^{(k)}$ (see also Fig. 2). In this case, (73) can be expressed as

$$\hat{\underline{\boldsymbol{d}}} = \underline{\boldsymbol{X}}\,\underline{\boldsymbol{Y}}\left[\underline{\boldsymbol{y}}^{(1,1)T} \cdots \underline{\boldsymbol{y}}^{(1,K_d^{(1)})T} \bullet\bullet\bullet \underline{\boldsymbol{y}}^{(K,1)T} \cdots \underline{\boldsymbol{y}}^{(K,K_d^{(K)})T}\right]^T \tag{78}$$

where $\underline{\boldsymbol{X}}$ and $\underline{\boldsymbol{Y}}$ are given by (69) and (77), respectively. The combination of the BF for the user k and its k_dth DOA with the DMF to user k and its k_dth DOA can be designated as a spatial decorrelating matched filter (SDMF) (see also Section IV). The outputs of the SDMF's that correspond to each user are combined according to the maximal ratio combining (MRC) strategy [25]. Finally, the outputs of the MRC's are fed into the ISI and MAI canceller [27], which removes intersymbol and

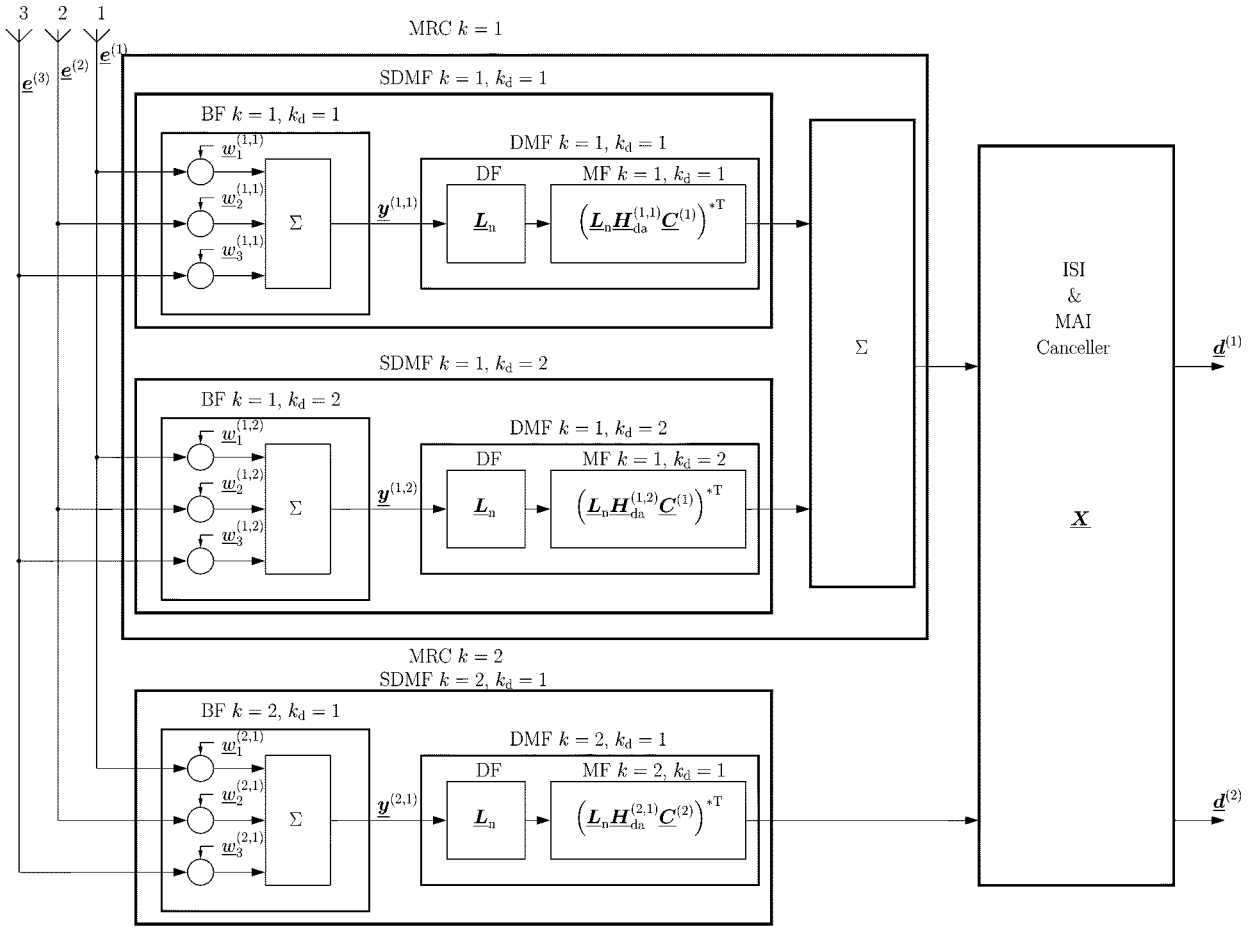

Fig. 5. Implementation of the novel joint data detector for the case of $K = 2$ users and $K_a = 3$ array elements.

multiple-access interference. The realization of this novel joint data detector is illustrated in Fig. 5 for the case of

$$K_a = 3, \quad K = 2, \quad K_d^{(1)} = 2, \quad K_d^{(2)} = 1. \tag{79}$$

VI. Simulation Results

In this section, the novel smart antenna concept presented in the paper is evaluated by simulations for the uplink of a TD-CDMA mobile radio system. This evaluation takes place in two steps. In a first step, the performance of the combined DOA and joint channel estimation, presented in Section IV, is compared to the conventional scheme for different scenarios in the rural and urban propagation environment. In a second step, the average bit error rate (BER) is investigated by Monte Carlo simulations of data transmission for a single cell and for different scenarios in the rural and urban propagation environment as a function of the average SNR E_b/N_0 per net information bit with respect to a single receiver antenna. The additive noise $\underline{\boldsymbol{n}}$ (see Section II), which could be caused by intercell interference in the interference-limited case, is assumed to be white and Gaussian distributed with zero mean, i.e., the link level system performance is evaluated. The noise covariance matrices for the channel estimation and the joint data detection [see (29) and (30)], respectively, are assumed to be

$$\underline{\boldsymbol{R}}_m = \sigma^2 \cdot \boldsymbol{I}^{(K_a L)} \tag{80}$$

$$\underline{\boldsymbol{R}}_n = \sigma^2 \cdot \boldsymbol{I}^{(K_a(NQ+W-1))} \tag{81}$$

where σ^2 is the variance of the noise of every array element, i.e., white and uncorrelated noise for the different antennas is considered. The value of σ^2 is calculated according to

$$\sigma^2 = \frac{N_0}{T_c} \tag{82}$$

where T_c is the chip duration and $N_0/2$ is the one-sided power spectral density of the additive white noise [28]. In the simulations, a ULA of eight array elements is used. The array elements are spaced at 0.5 of the carrier wavelength. Due to the limited directional resolution of a ULA parallel to the axis of the array, only a sector of 90° towards the broadside of the array is considered in the simulations. An azimuthal coverage of 360° is achieved by using URA's or cross arrays [29]. The main parameters of the TD-CDMA mobile radio system used for the simulations are given in [13]. It is noted that the user bandwidth B of 1.6 MHz is smaller than the inverse of the chip duration T_c. This results from the choice of a digital chip impulse filter having an impulse response equal to the GMSK basic impulse $C_0(\tau)$ of time bandwidth product 0.3, leading to a compact spectrum (see [13]). Furthermore, the digital chip impulse filter and the user specific spreading codes have been designed in such a way that the magnitude of the complex envelopes of the transmitted signals are approximately constant. Finally, it is to be noted that the real time implementation of the joint detection receiver can

already be achieved with today's hardware (see [30] for a detailed analysis).

Smart antenna concepts take advantage of the directional inhomogeneity of the mobile radio channel in order to increase the link level performance in mobile radio systems [4]. Thus, a performance evaluation of such system concepts should be based on channel models which, besides time variance and frequency selectivity, explicitly incorporate the directional inhomogeneity of the mobile radio channel [3]. In the simulations, each channel impulse response is the linear superposition of P uncorrelated echoes, each with a particular delay parameter represented by P sinusoids with equally distributed phase angles and Doppler frequencies according to the Jake spectrum [6], [31]. The delay parameters are exponentially distributed according to the delay power spectra associated with the desired propagation environment types [32], e.g., rural area (RA) and typical urban (TU). As in [6], P equal to 600 is chosen for the simulations. It is noted that the channel impulse responses generated according to this scheme exhibit the fast fading characteristics of the mobile radio channel, meaning that variations of the received power due to fast fading are present in the received signal, whereas variations due to path loss and shadowing are supposed to be perfectly eliminated by power control. In the case of the rural propagation environment the waves impinge on the BS within a small azimuthal range [3], [5], which can be approximated by a single DOA. For this reason, the channel models specified by COST207 [32] for transmission over RA are used, with the additional introduction of a single DOA for every user that is assigned to the considered BS. Since a ULA is employed at the BS, this is accomplished by multiplying the complex channel impulse responses created at a reference point of the array [6] by a complex exponential which is only dependent on the DOA of the channel impulse response and the array configuration. For the urban propagation environment, the channel models specified by COST207 for transmission over TU [32] are used. Different scenarios for the directional inhomogeneity of this environment type [5] are investigated by assigning $K_d^{(k)}, k = 1 \cdots K$, DOA's to the P aforementioned echoes (see also Section II). First, $K_d^{(k)}$ is chosen equal to two, which enables us to take upper bounds for the link level performance of a TD-CDMA mobile radio system in a TU propagation environment. Then, $K_d^{(k)}$ is increased to ten equidistant DOA's in an impinging range of 5° and 10°, modeling thus an angular spread (AS), which is a realistic situation in such propagation environment types [4], [5].

A. Performance of the Channel Estimation

In this section, the enhanced joint channel estimation is compared with the conventional channel estimation for the rural and the urban propagation environment. Fig. 6 shows the normalized root mean square error (RMSE) of the estimated combined channel impulse response $\hat{\underline{\boldsymbol{h}}}$ [see (31)] and the estimated directional combined channel impulse response $\hat{\underline{\boldsymbol{h}}}_d$ [see (44)], compared with the actual $\underline{\boldsymbol{h}}$ of (14), versus the average SNR E_b/N_0 per net information bit for the COST207 RA channel models, where a single DOA for each of the $K = 8$ simultaneously active users is employed. We note that after the implementation of (44), (7) is applied, enabling thus the comparison of the

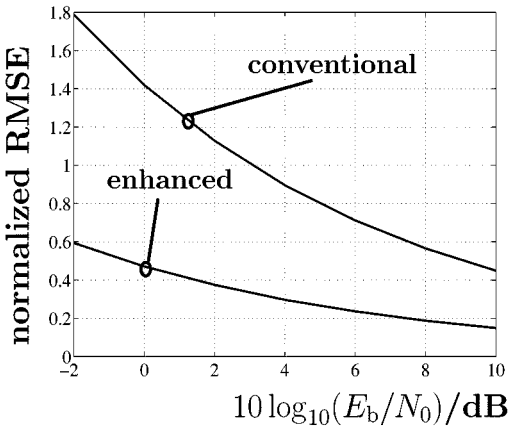

Fig. 6. Normalized RMSE; $K = 8$; COST207 RA; 90° DOA sector; uniformly distributed DOA's; $v = 90$ km/h; 500 bursts.

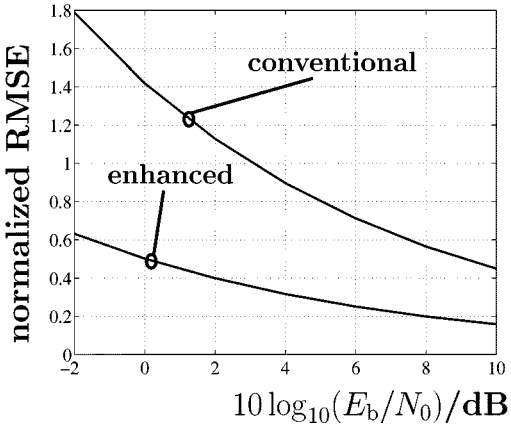

Fig. 7. Normalized RMSE; $K = 8$; COST207 RA; 90° DOA sector; users with the same DOA; $v = 90$ km/h; 500 bursts.

conventional and the enhanced joint channel estimation. The DOA's are uniformly distributed in a sector of 90° towards the broadside of the ULA. The number of impinging DOA's are estimated according to the modified minimum description length (MDL) criterion for centro-symmetric array configurations [33] and the DOA's themselves are estimated by the 1-D Unitary ESPRIT algorithm [18], [24]. Even if the number and the values of DOA's are assumed perfectly known at the BS receiver, the performance of the enhanced channel estimation is practically the same compared to the case when the number and the values of DOA's are estimated, since only one DOA per user is employed, cf. [24]. The first burst of the frame is considered (see Fig. 1), the velocity v equals 90 km/h, and the results are averaged over 500 transmitted bursts for every user. In Fig. 7, the investigated scenario involves the extreme case where all user signals are incident on the BS array from the same DOA. These results show the improvement achieved by the enhanced joint channel estimation for the rural propagation environment. This improvement is more obvious when the SNR takes small values, i.e., below 0 dB. Moreover, there is no performance degradation when the signals from the different users are incident on the BS array from the same DOA. This is due to the fact that

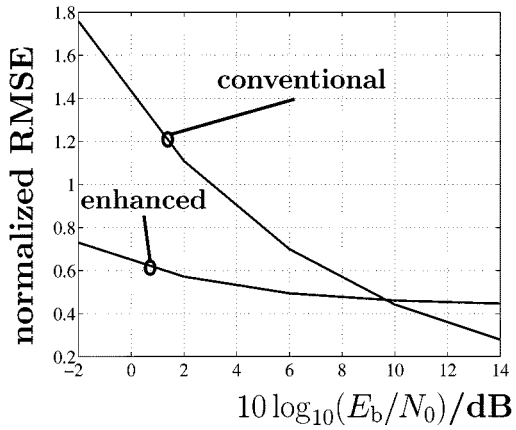

Fig. 8. Normalized RMSE; $K = 8$; COST207 TU; 90° DOA sector; AS = 5°; $v = 30$ km/h; 500 bursts.

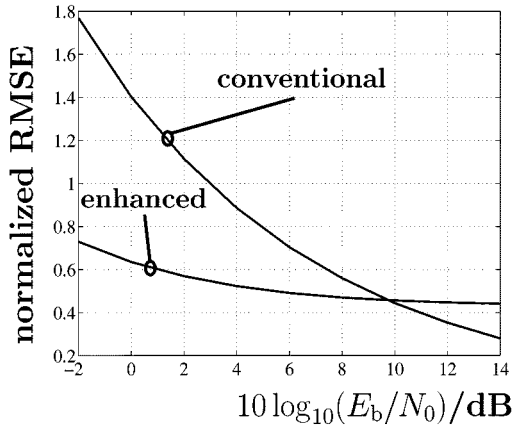

Fig. 9. Normalized RMSE; $K = 8$; COST207 TU; 90° DOA sector; AS= 10°; $v = 30$ km/h; 500 bursts.

the conventional joint channel estimation provides separate estimates for the channel impulse responses of the different users [see (33)]. Therefore, the user specific DOA processes perform independently of the values for the user DOA's and the enhanced joint channel estimation improves considerably the channel impulse response estimates. It is noted, though, that the BER performance is severely degraded when the user signals impinge from the same DOA, as it will be seen in Section VI-B.

Figs. 8 and 9 show the normalized RMSE of the estimated channel impulse responses $\hat{\underline{\boldsymbol{h}}}$ [see (31)] and $\hat{\underline{\boldsymbol{h}}}_d$ [see (44)] versus the average SNR E_b/N_0 per net information bit for the COST207 TU channel models, where an angular spread of 5° and 10° is employed, respectively. The first burst of the frame is considered (see Fig. 1) the velocity v equals 30 km/h, and the results are averaged over 500 transmitted bursts for every user. In this scenario, the number of the impinging signals $K_d^{(k)}$ (see Section II) is equal to ten and, moreover, they are restricted in a small azimuthal range of 5° and 10°, respectively. The angle of the line connecting each mobile to the BS is chosen to be in the center of said azimuthal range and the impinging signals $K_d^{(k)}$, $k = 1 \cdots K$, are assumed to be equally spaced within this range. Under these assumptions, a ULA with eight

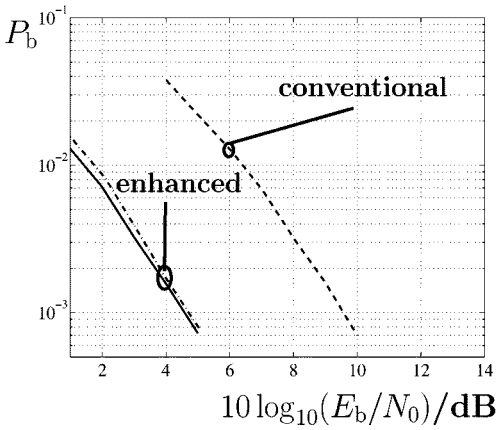

Fig. 10. P_b versus E_b/N_0; propagation environment: rural area COST207, single DOA's equidistant in a 90° sector; mobile speed: 90 km/h.

array elements cannot resolve all impinging signals. Moreover, even if we used a ULA with more array elements than eight, it would still not suffice for resolving all the signals, because they are within a small range (see also [24]). Therefore, the dominant DOA is estimated, i.e., the number of impinging signals is taken to be equal to one. Under these considerations, we observe that the enhanced joint channel estimation improves the channel impulse response estimates only in scenarios of small SNR's. When the SNR is sufficiently high, the conventional scheme performs better, since the one directional channel impulse response vector estimated by the enhanced scheme does not provide a more reliable estimate than the one from the conventional scheme for the ten impinging signals restricted in the angular spread of 5° or 10°. Despite this fact, the implementation of the enhanced scheme is still reasonable because in this propagation environment low values of the BER are achieved already at small values of the SNR. This system behavior is illustrated in Section VI-B.

B. Bit Error Rate Performance

In this section and according to the simulation environment described above, Monte Carlo simulations of data transmission are used to analyze the BER performance in the uplink of TD-CDMA mobile radio system for the enhanced receiver presented in this paper and the conventional receiver (see Sections IV and V). The average coded BER P_b is investigated for a single cell and for different scenarios in the rural and the urban propagation environment as a function of the average SNR E_b/N_0 per net information bit with respect to a single receiver antenna.

In Figs. 10–12, the channel models specified by COST207 RA [32] are used and it is assumed that a single DOA is assigned to every of the $K = 8$ simultaneously active users of the considered cell. The conventional receiver and the enhanced receiver with perfectly known DOA's (solid line) and estimated DOA's (dashed line) are considered. In Fig. 10, all user DOA's are equidistant in the 90° sector, which is the best possible spatial separation between the DOA's of the different users and offers the possibility to take upper bounds for the link level performance of a TD-CDMA mobile radio system in the rural

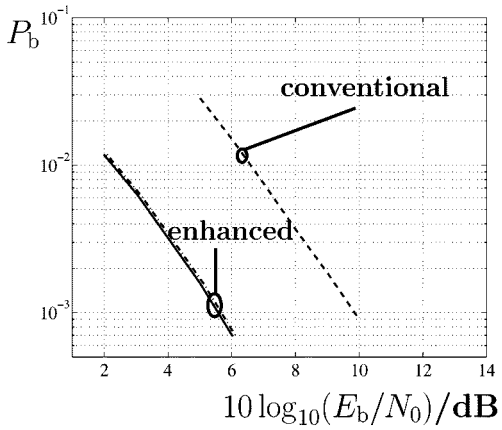

Fig. 11. P_b versus E_b/N_0; propagation environment: rural area COST207, single DOA's uniformly distributed in a 90° sector; mobile speed: 90 km/h.

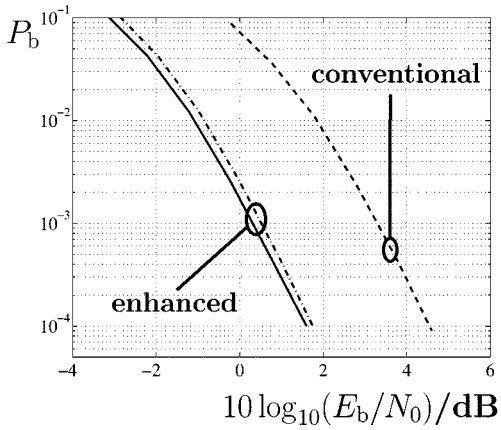

Fig. 13. P_b versus E_b/N_0; propagation environment: typical urban area COST207, two DOA's per user in a 90° sector; mobile speed: 30 km/h.

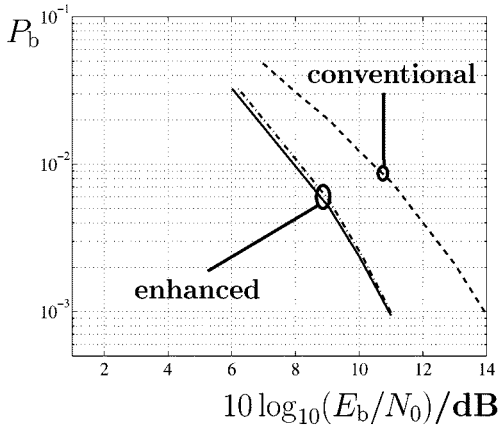

Fig. 12. P_b versus E_b/N_0; propagation environment: rural area COST207, same DOA for all users; mobile speed: 90 km/h.

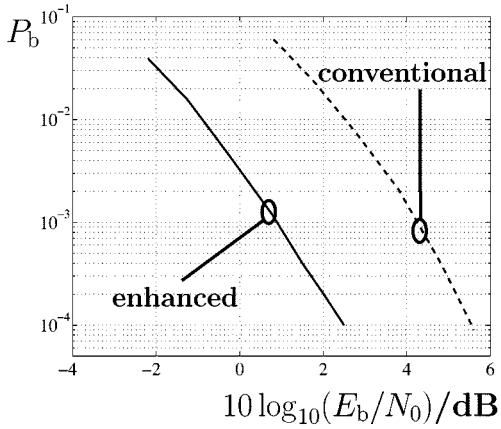

Fig. 14. P_b versus E_b/N_0; propagation environment: typical urban COST207, AS = 5° per user in a 90° sector; mobile speed: 30 km/h.

propagation environment. In Fig. 11, all user DOA's are uniformly distributed in the 90° sector, which is a realistic case for this propagation environment. Furthermore, the extreme case where all users have the same DOA is investigated in Fig. 12. The E_b/N_0 improvement due to the application of the enhanced receiver is approximately 5 dB at a BER of $P_b = 10^{-3}$ when the user DOA's are equidistant in the considered 90° sector (see Fig. 10). Since we refer to a channel model with single DOA's, and the noise on the array elements is assumed to be uncorrelated, the modified MDL criterion [33] and 1-D Unitary ESPRIT [24] provide estimates with increased accuracy (see also Section VI-A). Therefore, the link level performance is slightly degraded when the number and the values of DOA's are estimated and the improvement of the E_b/N_0 due to the application of the enhanced receiver still holds. In Fig. 11, where the DOA's are uniformly distributed, the system performance is slightly degraded compared to Fig. 10, where the DOA's are equidistant in the 90° sector, and the E_b/N_0 improvement due to the application of the enhanced receiver is also approximately 5 dB at a BER of $P_b = 10^{-3}$. Fig. 12 shows that the performance of systems with smart antennas can be severely degraded when the user signals impinge on the BS receiver from DOA's that are not well spatially separated. Here, the extreme case where all user signals impinge from the same DOA is investigated. In this scenario, the E_b/N_0 improvement due to the application of the enhanced receiver is 3 dB at a BER of $P_b = 10^{-3}$ compared to the conventional receiver, whereas the performance of both receivers is degraded approximately 6 and 4 dB, respectively. This simulation result can be justified by the existence of the DOA specific BF's in the novel joint data detector (see Fig. 5). When the DOA's of the simultaneously active users are not well spatially separated, although the quality of the channel estimation is not affected (see Fig. 7), the BF's in the joint data detector may receive a considerable amount of energy associated with the other DOA's of the same user and the DOA's of the other users, thus leading to a reduced quality for the joint data detection. In such scenarios, the system performance of a TD-CDMA mobile radio system can be kept close to the performance of Figs. 10 and 11 if a channel assignment strategy for the users active in the same frame is implemented (see [29] for a detailed analysis).

In Figs. 13–15, the average coded BER P_b is investigated for a single cell and for different scenarios in the TU COST207 propagation environment as a function of the average SNR E_b/N_0

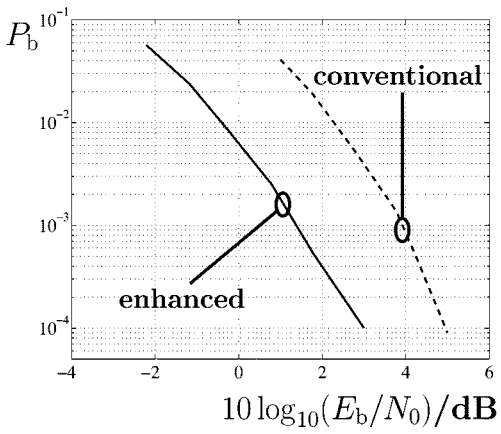

Fig. 15. P_b versus E_b/N_0; propagation environment: typical urban COST207, AS $= 10^\circ$ per user in a 90° sector; mobile speed: 30 km/h.

per net information bit with respect to a single receiver antenna. The conventional receiver and the enhanced receiver are considered. In Fig. 13, two DOA's in the 90° sector are assigned to every user. The conventional receiver and the enhanced receiver with perfectly known DOA's (solid line) and estimated DOA's (dash-dotted line) are considered. The number of DOA's are estimated by the MDL criterion [33] and the DOA's themselves by the 1-D Unitary ESPRIT algorithm [18]. The E_b/N_0 improvement due to the application of the enhanced receiver is approximately 3 dB at a BER of $P_b = 10^{-4}$, whereas the E_b/N_0 difference between the enhanced receiver with perfectly known and estimated DOA's does not exceed 0.5 dB. This result can be considered as an upper bound for the link level performance of a TD-CDMA mobile radio system in the TU COST207 propagation environment. In the more realistic scenario of Fig. 14, where there is an angular spread of 5° for every user assigned to the considered BS, the performance of the enhanced receiver is slightly degraded, whereas the improvement compared to the conventional scheme still holds. If the angular spread takes the larger value of 10° (see Fig. 15), then the performance of the enhanced receiver degrades approximately 0.5 dB compared to the case when the angular spread is 5° (see Fig. 14). However, the enhanced receiver offers a better performance in comparison with the conventional scheme, a fact that demonstrates the increased potential for performance enhancement of the novel scheme presented in this paper. As discussed in Section VI-A (see Figs. 8 and 9), the improved channel estimation of the conventional scheme takes place only at high SNR's and does not affect the BER performance, which reaches, e.g., a value of 10^{-4} for P_b already at low SNR's.

VII. Conclusions

In this paper, a combined DOA and joint channel estimation scheme for a time-slotted CDMA mobile radio system with joint detection has been presented. In a first step, the received signals from each array element are fed into a conventional joint channel estimator. In a second step, the channel impulse responses for the connections between each user and each array element are processed by user specific DOA estimators. In a final step, the channel impulse responses associated with the DOA's of each user are estimated. Moreover, a novel joint data detection technique, which explicitly takes into account the DOA's of signals carrying information and the associated directional channel impulse responses, is presented. This smart antenna concept is evaluated by simulations in the uplink of a TD-CDMA mobile radio system, which has been selected by ETSI to form part of the UMTS air interface standard. Different scenarios for the directional inhomogeneity of the mobile radio channel have been investigated in rural and urban propagation environments. The simulation results indicate that, depending on the propagation environment, considerable performance improvements are possible, due to the exploitation of the knowledge of the DOA's and the associated channel impulse responses.

References

[1] J. Fuhl and A. F. Molisch, "Capacity enhancement and BER in a combined SDMA/TDMA system," in *Proc. IEEE 46th Int. Veh. Technol. Conf. (VTC'96)*, Atlanta, GA, pp. 1481–1485.

[2] P. C. F. Eggers, "Angular dispersive mobile radio environments sensed by highly directive base station antennas," in *Proc. IEEE 6th Int. Symp. Personal, Indoor and Mobile Radio Communications (PIMRC'95)*, Toronto, Canada, pp. 522–526.

[3] J. J. Blanz, M. Haardt, A. Papathanassiou, I. Furió, and P. Jung, "Combined direction of arrival and channel estimation for time-slotted CDMA," in *Proc. 4th Int. Conf. Telecommunications (ICT'97)*, Melbourne, Australia, pp. 395–400.

[4] J. J. Blanz, P. W. Baier, and P. Jung, "A flexibly configurable statistical channel model for mobile radio systems with directional diversity," in *Proc. 2nd ITG Conf. Mobile Kommunikation*, Neu-Ulm, 1995, pp. 93–100.

[5] A. Klein, W. Mohr, R. Thomas, P. Weber, and B. Wirth, "Direction-of-arival of partial waves in wideband mobile radio channels for intelligent antenna concepts," in *Proc. IEEE 46th Int. Veh. Technol. Conf. (VTC'96)*, Atlanta, GA, pp. 849–853.

[6] P. Jung and J. J. Blanz, "Joint detection with coherent receiver antenna diversity in CDMA mobile radio systems," *IEEE Trans. Veh. Technol.*, vol. 44, pp. 76–88, 1995.

[7] A. Klein and P. W. Baier, "Simultaneous cancellation of cross interference and ISI in CDMA mobile radio communications," in *IEEE Proc. 3rd Int. Symp. Personal, Indoor and Mobile Radio Communications (PIMRC'92)*, Boston, MA, pp. 118–122.

[8] ——, "Linear unbiased data estimation in mobile radio systems applying CDMA," *IEEE J. Select. Areas Commun.*, vol. 11, pp. 1058–1066, 1993.

[9] A.-J. van der Veen, M. C. Vanderveen, and A. Paulraj, "Joint angle and delay estimation using shift-invariance properties," *IEEE Signal Processing Lett.*, vol. 4, pp. 142–145, 1997.

[10] ——, "Joint angle and delay estimation using shift-invariance techniques," *IEEE Trans. Signal Processing*, vol. 46, no. 2, pp. 405–418, 1998.

[11] M. C. Vanderveen, C. Papadias, and A. Paulraj, "Joint angle and delay estimation (JADE) for multipath signals arriving at an antenna array," *IEEE Commun. Lett.*, vol. 1, no. 1, pp. 12–14, 1997.

[12] P. Jung, P. W. Baier, and A. Steil, "Advantages of CDMA and spread spectrum techniques over FDMA and TDMA in cellular mobile radio applications," *IEEE Trans. Veh. Technol.*, vol. 42, pp. 357–364, 1993.

[13] J. J. Blanz, A. Klein, M. Naßhan, and A. Steil, "Performance of a cellular hybrid C/TDMA mobile radio system applying joint detection and coherent receiver antenna diversity," *IEEE J. Select. Areas Commun.*, vol. 12, pp. 568–579, 1994.

[14] *ETSI/TC GSM Recommendations, 01-12*, 1988.

[15] A. Papathanassiou, M. Haardt, I. Furió, and J. J. Blanz, "Multi-user direction of arrival and channel estimation for time-slotted CDMA with joint detection," in *IEEE Proc. Int. Conf. Digital Signal Processing (DSP'97)*, pp. 375–378.

[16] B. Steiner and P. Jung, "Optimum and suboptimum channel estimation for the uplink of CDMA mobile radio systems with joint detection," *European Trans. Telecommun. Related Techniques*, vol. 5, pp. 39–50, 1994.

[17] R. Roy and T. Kailath, "ESPRIT—Estimation of signal parameters via rotational invariance techniques," *IEEE Trans. Acoust., Speech, Signal Processing*, vol. 37, pp. 984–995, 1989.
[18] M. Haardt and J. A. Nossek, "Unitary ESPRIT: How to obtain increased estimation accuracy with a reduced computational burden," *IEEE Trans. Signal Processing*, vol. 43, pp. 1232–1242, 1995.
[19] A. Graham, *Kronecker Products and Matrix Calculus: With Applications*. Chichester, U.K.: Ellis Horwood, 1981.
[20] G. Calhoun, *Digital Cellular Radio*. Norwood, MA: Artech, 1988.
[21] W. C. Y. Lee, *Mobile Cellular Telecommunications Systems*. New York: McGraw-Hill, 1989.
[22] A. Klein, "Multi-user detection of CDMA-signals—Algorithms and their application to cellular mobile radio," in *Fortschrittberichte VDI*. Düsseldorf, Germany: VDI-Verlag, 1996, vol. 10.
[23] A. D. Whalen, *Detection of Signals in Noise*. New York: Academic, 1971.
[24] M. Haardt, *Efficient One-, Two-, and Multidimensional High-Resolution Array Signal Processing*. Aachen, Germany: Shaker Verlag, 1996.
[25] R. A. Monzingo and W. T. Miller, *Introduction to Adaptive Arrays*. New York: Wiley, 1980.
[26] P. Jung, F. Berens, J. Blanz, and J. Plechinger, "Performance of multicarrier joint detection CDMA mobile communication systems," in *Proc. IEEE 47th Int. Veh. Technol. Conf. (VTC'97)*, Phoenix, AZ, pp. 1892–1896.
[27] R. Kohno, H. Imai, M. Hatori, and S. Pasupathy, "An adaptive canceller of co-channel interference for spread spectrum multiple access communication networks in a power line," *IEEE J. Select. Areas Commun.*, vol. 8, pp. 641–649, 1990.
[28] J. G. Proakis, *Digital Communications*, 2nd ed. New York: McGraw-Hill, 1989.
[29] A. Papathanassiou, J. J. Blanz, M. Haardt, and P. W. Baier, "Spatial channel assignment considerations in a joint detection CDMA mobile radio system employing smart antennas," in *Proc. 5th Int. Conf. Telecommunications (ICT'98)*.
[30] J. Mayer, J. Schlee, and T. Weber, "Realtime feasibility of joint detection CDMA," in *Proc. 2nd European Personal Mobile Communications Conf. (EPMCC'97)*, Bonn, Germany, pp. 245–252.
[31] P. Höher, "A statistical discrete-time model for the WSSUS multipath channel," *IEEE Trans. Veh. Technol.*, vol. 41, pp. 461–468, 1992.
[32] "COST207, digital land mobile radio communications," Office for Official Publications of the European Communities, Luxembourg, Final Rep., 1989.
[33] G. Xu, R. H. Roy, and T. Kailath, "Detection of number of sources via exploitation of the centro-symmetry property," *IEEE Trans. Acoust., Speech, Signal Processing*, vol. 42, pp. 102–112, 1994.

Josef Johannes Blanz received the M.S.E.E. (Dipl.-Ing.) and Ph.D. (Dr.-Ing.) degrees in electrical engineering from the University of Kaiserslautern, Kaiserslautern, Germany, in 1993 and 1998, respectively.

From 1990 to 1992, he was a Freelance Coworker with the Microelectronics Centre, University of Kaiserslautern, where he was engaged in the design of digital communication circuits. In 1993, he joined the Research Group for RF Communications, University of Kaiserslautern, as a Research Engineer, focusing on future mobile radio systems with special emphasis on antenna diversity and smart antenna techniques for CDMA. Since 1998, he has been with Qualcomm, Inc., Boulder, CO, where he is developing smart antenna solutions for CDMA and third-generation mobile radio standards.

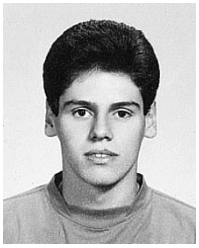

Apostolos Papathanassiou received the diploma in electrical engineering and computer sciences from the National Technical University of Athens (NTUA), Greece, in 1994. He is currently working towards the Ph.D. degree.

From January 1995 to July 1996, he served in the Greek Army, where he specialized in telecommunications. In August 1996, he joined the Research Group for RF Communications at the University of Kaiserslautern, Kaiserslautern, Germany, as a Research Engineer. His research interests are in smart antennas for mobile radio systems, spread-spectrum techniques, and statistical signal processing.

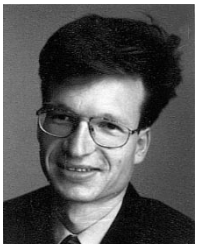

Martin Haardt (S'90–M'98–SM'99) was born in Germany on October 4, 1967. He received the Diplom-Ingenieur (M.S.) degree from the Ruhr-University Bochum, Germany, in 1991 and the Doktor-Ingenieur (Ph.D.) degree from the Munich University of Technology, Germany, in 1996, both in electrical engineering.

From 1989 to 1990, he was a Visiting Scholar at Purdue University, West Lafayette, IN, sponsored by a fellowship from the German Academic Exchange Service (DAAD). From 1991 to 1993, he was with Corporate Research and Development, Siemens AG, Munich, Germany, conducting research in the areas of image processing and biomedical signal processing. From 1993 to 1996, he was a Research Associate with the Institute of Network Theory and Circuit Design at the Munich University of Technology, where his research was focused on smart antennas. In 1997, he joined Siemens Mobile Networks, Munich, where he was responsible for strategic research for third-generation mobile radio systems. Since 1998, he has been serving as Director of International Projects and University Projects in the Chief Technical Office of Siemens Communication on Air. He also teaches at the Munich University of Technology. He is a contributing author to *The Digital Signal Processing Handbook* (New York: IEEE Press, 1998). His current research interests include wireless communications, array signal processing, digital signal processing, and numerical linear algebra.

Dr. Haardt received the Rohde & Schwarz Outstanding Dissertation Award in 1997 for his Ph.D. dissertation. In 1998, he was the corecipient of the Mannesmann Mobilfunk Innovations Award for outstanding research in mobile communications. He also received the ITG Best Paper Award from the Information Technology Society (ITG) of the Association of Electrical Engineering, Electronics, and Information Technology (VDE). He is a member of the Association of Electrical Engineering, Electronics, and Information Technology (VDE).

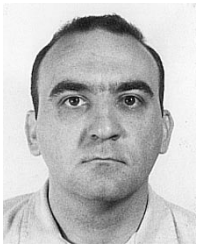

Ignasi Furió (SM'95) was born in Palma de Mallorca, Spain, on February 8, 1963. He received the Engineer of Telecommunications degree from the Universitat Politècnica de Catalunya (UPC), Spain, in 1992. He is currently working towards the Ph.D. degree in electrical engineering at the Universitat de les Illes Balears (UIB), Palma de Mallorca.

In 1997, he was invited to join the Research Group for RF Communications at the University of Kaiserslautern, Kaiserslautern, Germany, for six months as a Research Engineer. His research interests are in spread-spectrum communications and TCM.

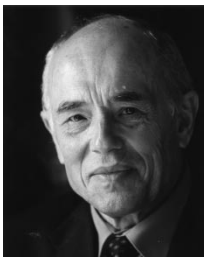

Paul Walter Baier (F'95) was born in Backnang, Germany, in 1938 and graduated from the Technical University Munich, Germany.

At the Technical University Munich, he was a Senior Lecturer until 1970. In 1970, he joined the Central Telecommunications Laboratories of Siemens AG, Munich, where he became Head of the Spread Spectrum Development Group and was engaged in various topics of communication engineering. Since 1973, he has been a Professor of Electrical Communications and Director of the Institute for RF Communications and Fundamentals of Electronic Engineering at the University of Kaiserslautern, Kaiserslautern, Germany. His main research interests are spread-spectrum techniques, impulse compression radars, imaging radars, mobile radio systems, and adaptive antennas. The basics of the TD-CDMA component of the UMTS Terrestrial Radio Access System (UTRA) adapted by ETSI in January 1998 and also forming part of the IMT-2000 standard agreed upon by 3 GPP were developed by him in cooperation with Siemens. He coauthored two books and over 100 papers and supervised over 40 Ph.D. candidates.

Dr. Baier is a member of the U.R.S.I. Member Committee Germany. He received the Innovation Prize 1999 from the Mannesmann Mobile Radio Foundation.